Seventh International Conference on Computational Fluid Dynamics (ICCFD7), Big Island, Hawaii, July 9-13, 2012

ICCFD7-2102

Accurate Sharp Interface Scheme for Multimaterials

Y. Gorsse*, A. Iollo*, T. Milcent**, H. Telib***
Corresponding author: thomas.milcent@u-bordeaux1.fr

* Univ. Bordeaux, IMB, UMR 5251, F-33400 Talence, France.
CNRS, IMB, UMR 5251, F-33400 Talence, France.
INRIA, F-33400 Talence, France.
** Univ. Bordeaux, ENSAM-I2M, UMR CNRS 5295,33607 Pessac, France.
***Dipartimento di Ingegneria Aeronautica e Spaziale,
Politecnico di Torino, and Optimad Engineering,
Via Giacinto Collegno 18, 10143 Turin, Italy.

Abstract: We present a method to capture the evolution of a contact discontinuity separating two different material. A locally non-conservative scheme allows an accurate and stable simulation while the interface is kept sharp. Numerical illustrations include problems involving fluid and elastic problems.

Keywords: Multimaterial scheme, Sharp interface, Second Order.

1 Introduction

Physical and engineering problems that involve several materials are ubiquitous in nature and in applications: multi-phase flows, fluid-structure interaction, particle flows, to cite just a few examples. The main contributions in the direction of simulating these phenomena go back to [1] and [2]. The idea is to model the eulerian stress tensor through a constitutive law reproducing the mechanical characteristics of the medium under consideration. Hence, for example, an elastic material or a gas will be modeled by the same set of equations except for the constitutive law relating the deformation and the stress tensor. The system of conservation laws thus obtained can be cast in the framework of quasi-linear hyperbolic partial differential equations (PDEs). From the numerical view point this is convenient since classical integration schemes can be employed in each material. However, it turns out that the evolution of the interface, which is represented in this model by a contact discontinuity, is particularly delicate because standard Godunov schemes fail. In [3] it was shown that a simple and effective remedy to this problem is the definition of a ghost fluid across the interface. A remarkable application based on this approach is presented in [4]. This method, however, has the disadvantage that the interface is diffused over a certain number of grid points. From a practical view point this can be a serious drawback if one is interested in the geometric properties of the evolving interface, as, for example, in the case of surface tension or when the interface itself is elastic. In [5], we developed a first order scheme for multimaterial. In this paper we further explore the model and propose a simple second-order accurate method based on the ideas developped in [6].

2 The model

This approach was discussed in [1], [2], [7] and [4]. We develop here the principal elements of the formulation. The starting point is classical continuum mechanics. Let $\Omega_0 \subset \mathbb{R}^3$ be the reference or initial configuration of a single material and $\Omega_t \subset \mathbb{R}^3$ the deformed configuration at time t. We define $X(\xi, t)$ as the image at time t of a material point ξ belonging to the initial configuration, in the deformed configuration, i.e., $X : \Omega_0 \times [0, T] \longrightarrow \Omega_t$, $(\xi, t) \mapsto X(\xi, t)$, and the corresponding velocity field u as $u : \Omega_t \times [0, T] \longrightarrow \mathbb{R}^3$,

$(x,t) \mapsto u(x,t)$ where $X_t(\xi,t) = u(X(\xi,t),t)$ completed by the initial condition $X(\xi,0) = \xi$. Also we introduce the backward characteristics $Y(x,t)$ that for a time t and a point x in the deformed configuration, gives the corresponding initial point ξ in the initial configuration, i.e., $Y : \Omega_t \times [0,T] \longrightarrow \Omega_0$, $(x,t) \mapsto Y(x,t)$ with the initial condition $Y(x,0) = x$. Of course, since $Y(X(\xi,t),t) = \xi$ we have $[\nabla_\xi X(\xi,t)] = [\nabla_x Y(x,t)]^{-1}$ and $Y_t + (u \cdot \nabla_x)Y = 0$.

In Lagrangian elasticity, the internal energy per unit volume W is a function of the strain tensor $\nabla_\xi X$ and the entropy s

$$\mathcal{E} = \int_{\Omega_0} W(\nabla_\xi X(\xi,t), s(X(\xi,t),t))d\xi \tag{1}$$

The first Piola Kirchoff tensor $\mathcal{T}$ is defined as

$$\mathcal{T}(\xi,t) = \frac{\partial W}{\partial F}\Big|_{s=cte}(\nabla_\xi X, s(X,t)) \tag{2}$$

and the entropy is just transported along the characteristics if the velocity is smooth (no shocks). The potential W has to be Galilean invariant. Also, in this paper we focus on the isotropic case. It can be proven that (Rivlin-Eriksen theorem [8]) the potentiol is Galilean invariant and isotropic if, and only if, W is expressed as a function of the entropy, and of the invariants of the right Cauchy-Green tensor $C(\xi,t) = [\nabla_\xi X]^T[\nabla_\xi X]$ which are the same of $B(\xi,t) = [\nabla_\xi X][\nabla_\xi X]^T$. The invariants often considered in the literature are $J(\xi,t) = \det([\nabla_\xi X])$, $\mathrm{Tr}(C(\xi,t))$ and $\mathrm{Tr}(\mathrm{Cof}(C(\xi,t)))$. We assume that W is the sum of W_{vol}, a term depending on volume variation and entropy , and W_{iso} a term accounting for isochoric deformation. In general the term relative to an isochoric transformation will also depend on entropy. Here, we will limit the discussion to materials where shear forces are conservative. The backward characteristics $Y(x,t)$ are the starting point of the Eulerian formulation of elasticity since they capture the deformations of the media and map the reference domain Ω_0 in the physical domain Ω_t. The internal energy is given in the deformed configuration by

$$\mathcal{E} = \int_{\Omega_t} \Big(W_{\mathrm{vol}}(J,s) + W_{\mathrm{iso}}(\mathrm{Tr}(\overline{B}), \mathrm{Tr}(\mathrm{Cof}(\overline{B}))\Big) J^{-1} dx \tag{3}$$

where

$$J(x,t) = \det([\nabla_x Y(x,t)])^{-1} \qquad B(x,t) = [\nabla_x Y(x,t)]^{-1}[\nabla_x Y(x,t)]^{-T} \qquad \overline{B}(x,t) = \frac{B(x,t)}{\det(B(x,t))^{\frac{1}{3}}} \tag{4}$$

It can be shown that $\sigma(x,t)$, the Cauchy stress tensor in the physical domain, is given by

$$\sigma(x,t) = W'_{\mathrm{vol}}(J,s)I + 2J^{-1}\left(\overline{\sigma}_{\mathrm{iso}} - \frac{\mathrm{Tr}(\overline{\sigma}_{\mathrm{iso}})}{3} I\right) \quad \text{with} \quad \overline{\sigma}_{\mathrm{iso}} = \frac{\partial W_{\mathrm{iso}}}{\partial a}\overline{B} - \frac{\partial W_{\mathrm{iso}}}{\partial b}\overline{B}^{-1}. \tag{5}$$

By definition pressure is given by $p = -\dfrac{1}{3}\mathrm{Tr}\,(\sigma) = -W'_{\mathrm{vol}}(J,s)$ where $'$ denote the differentiation with respect to the first variable.

The governing equations derived from the above formulation in the deformed configuration are:

$$\begin{cases} \rho_t + \mathrm{div}_x(\rho u) = 0 \\ (\rho u)_t + \mathrm{div}_x(\rho u \otimes u - \sigma) = 0 \\ (\nabla_x Y)_t + \nabla_x(u \cdot \nabla_x Y) = 0 \\ (\rho e)_t + \mathrm{div}_x(\rho e u - \sigma^T u) = 0 \end{cases} \tag{6}$$

The unknowns are the backward characteristics of the problem $Y(x,t)$, the velocity $u(x,t)$, the total energy per unit mass $e(x,t)$ and the density $\rho(x,t)$. The initial density $\rho(x,0)$, the initial velocity $u(x,0)$,

the initial total energy $e(x,0)$ and $\nabla_x Y(x,0) = I$ are given together with boundary conditions.

For the objectives of this paper, we restrict our investigation to an elastic two-dimensional case. The constitutive law considered in this paper is given by the following internal energy per unit mass $\varepsilon = W/\rho_0$

$$\varepsilon = e - \frac{1}{2}|u|^2 = \frac{\kappa(s)\rho^{\gamma-1}}{\gamma-1} + \frac{p_\infty}{\rho} + \frac{\chi}{\rho_0}(\mathrm{Tr}\,(\overline{B}) - 2) \tag{7}$$

where $\kappa(s) = e^{\frac{s-s_0}{c_v}}$ and $\gamma,\ p_\infty, \chi \in \mathbb{R}^+$ are constants that characterize a given material. The two first terms represent a stiffened gas and the third concern a Neo Hookean elastic solid. This model accounts for elastic deformations in the transverse direction, i.e., $\sigma^{21} \neq 0$. The associated Cauchy stress tensor is given by

$$\sigma(x,t) = -(\kappa(s)\rho^\gamma - p_\infty)I + 2J^{-1}\chi\left(\overline{B} - \frac{\mathrm{Tr}(\overline{B})}{2}I\right) \tag{8}$$

where in two dimensions $\overline{B} = \dfrac{B}{\det(B)^{\frac{1}{2}}}$, so that $\det(\overline{B}) = 1$.

Let $x = (x_1, x_2)$ be the coordinates in the canonical basis of $\mathbb{R}^2$, $u = (u_1, u_2)$ the velocity components, $Y = (Y^1, Y^2)$ the components of Y and σ^{ij} the components of the stress tensor σ. Also, let us denote by $,i$ differentiation with respect to x_i. Our scheme is based on a directional splitting on a cartesian mesh. When computing the numerical fluxes at cell interfaces in the x_1 direction we have $(Y^1_{,2})_t = (Y^2_{,2})_t = 0$ thus $Y^1_{,2}$ and $Y^2_{,2}$ are constants. The governing equations in conservative form become

$$\Psi_t + (F(\Psi))_{,1} = 0$$

with $\phi_i = \rho u_i$ and $\psi = \rho e$

$$\Psi = \begin{pmatrix} \rho \\ \phi_1 \\ \phi_2 \\ Y^1_{,1} \\ Y^2_{,1} \\ \psi \end{pmatrix} \qquad F(\Psi) = \begin{pmatrix} \phi_1 \\ \frac{(\phi_1)^2}{\rho} - \sigma^{11} \\ \frac{\phi_1\phi_2}{\rho} - \sigma^{21} \\ \frac{\phi_1 Y^1_{,1} + \phi_2 Y^1_{,2}}{\rho} \\ \frac{\phi_1 Y^2_{,1} + \phi_2 Y^2_{,2}}{\rho} \\ \frac{\phi_1\psi - (\sigma^{11}\phi_1 + \sigma^{21}\phi_2)}{\rho} \end{pmatrix}$$

The numerical fluxes are computed with a HLLC approximate Riemann solver. This solver requires the analytical expression of the waves velocities which are the eigenvalues of the Jacobian of $F(\Psi)$. The waves velocities are defined locally by infinitesimal variation of the conservative variables. Therefore the energy equation can be replaced by the transport equation on the entropy $s_t + u \cdot \nabla s = 0$ and the wave velocities calculations are performed at fixed entropy. In the case of the constitutive law (7) there are 5 waves given by

$$\Lambda_E = \left\{ u_1, u_1 \pm \sqrt{\frac{\mathcal{A}_1 \pm \sqrt{\mathcal{A}_2}}{\rho}} \right\}$$

where

$$\mathcal{A}_1 = \chi((Y^1_{,1})^2 + (Y^2_{,1})^2 + (Y^1_{,2})^2 + (Y^2_{,2})^2) + \rho c^2(\rho, s)/2$$
$$\mathcal{A}_2 = (\chi((Y^1_{,2})^2 + (Y^2_{,2})^2 - (Y^1_{,2})^2 - (Y^2_{,2})^2) - \rho c^2(\rho, s)/2)^2 + 4\chi^2(Y^1_{,1}Y^1_{,2} + Y^2_{,1}Y^2_{,2})^2$$

and

$$c^2(\rho,s)=\frac{\partial p}{\partial \rho}\Big|_{s=cte}=\gamma\kappa(s)\rho^{\gamma-1}=\frac{\gamma(p+p_\infty)}{\rho}$$

is the classical speed of sound. These formulas are remarkable since they prove that the constitutive law (7) leads to an hyperbolic system for $\gamma, p_\infty, \chi > 0$ (we have $\mathcal{A}_1, \mathcal{A}_2 > 0$ and $\mathcal{A}_1 > \sqrt{\mathcal{A}_2}$) and we get the classical results of the stiffened gas model in the particular case $\chi = 0$.

2.1 Exact Riemann solver

A five-wave exact Riemann solver based on the method described in [9] is set up in order to validate the numerical scheme. This is an iterative method whose solution converges to the solution of the Riemann problem, i.e. system of equation (6) with the initial conditions

$$\Psi(x,t=0)=\left\{\begin{array}{l}\Psi_l \text{ if } x\leq x_0\\ \Psi_r \text{ if } x>x_0,\end{array}\right. \tag{9}$$

where x_0 is the position of the discontinuity at initial time. The solution of the Riemann problem is composed of six constant states separated by five distinct waves, which are from left to right: a normal stress wave, a transverse shear wave, a contact wave, a transverse shear wave and a normal stress wave, see Fig. 1. The solution across each wave is uniquely determined knowing the state on either side and the wave velocity.

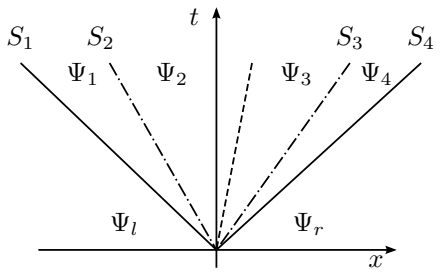

Figure 1: Representation of the Riemann problem for system (6). The constant states are denoted by Ψ_j, and the wavespeeds concerning the non-linear waves by S_j, $1 \leq j \leq 4$. The dashed line is the contact wave.

Given an initial estimate of each constant state, one determines the wave types and the wave speeds. Then, knowing the wave speeds, the left and right states Ψ_l and Ψ_r, and the wave types, one can determine the state across waves 1 and 5 using a Newton method, and so on for waves 2 and 3. Once a solution is found for states Ψ_2 and Ψ_3, the error concerning the continuity of the velocity and the stress tensor across the contact wave is calculated. This error is used to improve wave speeds estimates perturbating each wave speed, see [9] for a full description.

3 Numerical scheme

3.1 Multimaterial solver

We assume that the initial condition at time t_n, the n-th time step, is known. Let $\Psi_k^n = \Psi(x_k, t_n)$, with x_k the spatial coordinate x of grid point k. The discretization points are $N+1$ and let $I = \{1, \cdots, N\}$. Consider two non-miscible materials separated by a physical interface located, at time t_n, in x_f^n and let $\iota = i$ such that $x_i \leq x_f < x_{i+1}$, $i \in I$. At first order, the space and time discretization $\forall k \in I$ and $k \neq \iota, \iota+1$ is as follows

$$\frac{\Psi_k^{n+1}-\Psi_k^n}{\Delta t}=-\frac{\mathcal{F}_{k+1/2}^n(\Psi_k^n,\Psi_{k+1}^n)-\mathcal{F}_{k-1/2}^n(\Psi_{k-1}^n,\Psi_k^n)}{\Delta x} \tag{10}$$

where $\Delta t = t^{n+1} - t^n$, $\Delta x = x_{k+1/2} - x_{k-1/2}$ and $\mathcal{F}_{k\pm1/2}^n$ are the numerical fluxes evaluated at the cell interface located at $x_{k\pm1/2}$. For consistency $\mathcal{F}$ is a regular enough function of both arguments and $\mathcal{F}(\Psi,\Psi) = F(\Psi)$.

Numerical conservation requires that $\mathcal{F}(\Psi', \Psi) = \mathcal{F}(\Psi, \Psi')$. The numerical flux function $\mathcal{F}_{k+1/2}(\Psi_k^n, \Psi_{k+1}^n)$ is computed by an approximate Riemann solver. In the following we use the HLLC [10] approximate solver. The wave pattern involves five waves in the exact problem, but the HLLC approximate solver approaches the solution using three waves and thus defining two intermediate states Ψ_- and Ψ_+. The three waves are the contact discontinuity and the two fastest waves. Rankine Hugoniot conditions are used to determine the two intermediate states.

In any case, we assume that Riemann solver employed defines at least two intermediate states Ψ_-^n and Ψ_+^n, in addition to Ψ_k^n and Ψ_{k+1}^{n+1} and a contact discontinuity of speed u_*^n. The fluid speed is continuous across the states Ψ_-^n and Ψ_+^n. These states are defined so that mechanical equilibrium is ensured at the contact discontinuity.

Let us assume that Ψ_-^n is the state to the left of the contact discontinuity and Ψ_+^n to the right. The main idea is to use a standard numerical flux function $\mathcal{F}(\Psi_k, \Psi_{k+1})$, $\forall k \in I$, $k \neq \iota, \iota+1$ and from (10) to deduce Ψ_k^{n+1}. In contrast, for Ψ_ι^{n+1} and $\Psi_{\iota+1}^{n+1}$ we have

$$\begin{cases} \dfrac{\Psi_\iota^{n+1} - \Psi_\iota^n}{\Delta t} = -\dfrac{\mathcal{F}_-^n(\Psi_-^n) - \mathcal{F}_{\iota-1/2}^n(\Psi_{\iota-1}^n, \Psi_\iota^n)}{\Delta x} \\ \dfrac{\Psi_{\iota+1}^{n+1} - \Psi_{\iota+1}^n}{\Delta t} = -\dfrac{\mathcal{F}_{\iota+3/2}^n(\Psi_{\iota+1}^n, \Psi_{\iota+2}^n) - \mathcal{F}_+^n(\Psi_+^n)}{\Delta x} \end{cases} \tag{11}$$

where $\mathcal{F}_\pm^n = F(\Psi_\pm^n)$. The scheme is locally non conservative since $\mathcal{F}_+^n \neq \mathcal{F}_-^n$. However, the effect on the approximation of shocks is negligible. The interface position is updated in time using u_*^n, i.e., $x_f^{n+1} = x_f^n + u_*^n\, \Delta t$. For numerical stability, the integration step is limited by the fastest of the characteristics over the grid points. Hence, the interface position will belong to the same interval between two grid points for more than one time step. When the physical interface overcomes a grid point, i.e., $x_f^{n+1} \geq x_{i+1}$ or $x_f^{n+1} < x_i$ then $\iota = i \pm 1$ accordingly. In other words, the above integration scheme is simply shifted of one point to the right or to the left.

When the interface crosses a grid point, however, the corresponding conservative variables Ψ_ι^{n+1} do not correspond anymore to the material present at that grid point before the integration step. When $\iota = i+1$, i.e., the physical interface moves to the right of $i+1$, then we take $\Psi_\iota^{n+1} = \Psi_-^n$, whereas if $\iota = i-1$, $\Psi_\iota^{n+1} = \Psi_+^n$. The scheme proposed in [11] can be simplified and recast in a form similar to what we presented here.

3.2 Second order

To reach second order accuracy, a MUSCL slope reconstruction, see [12], is performed for the conservative variables, and a second order Runge Kutta time integration is used.

At the physical interface defined as the iso-line zero of a level set function, a Riemann problem is defined by extrapolation of the slopes, and the interface velocity $\mathbf{u}_{\text{int}}$ is defined as the contact discontinuity velocity. Once the velocity is known, the scheme presented in [6] can be applied in order to get a globally second order scheme.

Let Ψ_l^{prim} and Ψ_r^{prim} be the primitive variable vectors at the $i+1/2$ interface determined with the standard slope reconstruction. For th cells concerned by a sign change of the level set function, the following procedure is applied:

First case: the current cell is fluid ($\chi_i = 0$), the scheme [6] is applied without modification. To impose the interface velocity at second order accuracy, the velocity of the contact discontinuity $\mathbf{u}^*$ at the numerical interface is determined by:

$$\begin{aligned} u_1^* &= u_{1,\text{int}} + (d - 1/2) s_b \\ u_2^* &= u_{2,l} \end{aligned} \tag{12}$$

where d is the distance between the center of the current cell and the physical interface, and s_b is the slope of u_1 at the numerical interface, defined by (for example in the case of a sign change between i and $i+1$):

$$s_b = u_{1,\text{int}} - u_{1,i} + \frac{1-d}{1+d} \left(u_{1,\text{int}} - u_{1,i-1} \right). \tag{13}$$

If a slope limiter is needed, the limited slope is defined by $s_b^l = \text{minmod}(s_b, s_3)$, where $s_3 = u_{1,i} - u_{1,i-1}$.

Then, a fictitious state is created at the other side of the numerical interface such that the boundary condition is satisfied. Knowing the left state Ψ_l^{prim} thanks to the standard slope reconstruction of the variables u_1, u_2, $Y_{,1}^1$, $Y_{,1}^2$, $Y_{,2}^1$, $Y_{,2}^2$, p and c at the numerical interface, the right state is defined by:

$$\Psi_r^{\text{prim}} = (2u_1^* - u_1, u_2^*, Y_{,1}^1, Y_{,1}^2, Y_{,2}^1, Y_{,2}^2, p, c), \tag{14}$$

Second case: the current cell is a solid one ($\chi_i \neq 0$), the same scheme is applied as for the first case, but both of the components of the interface velocity are imposed in the same manner:

$$\mathbf{u}^* = \mathbf{u}_{\text{int}} + (d - 1/2)\mathbf{s}_b, \tag{15}$$

where $\mathbf{u}^* = (u_1^*, u_2^*)$ and $\mathbf{s}_b$ is a two component slope concerning the velocity at the interface, calculated using the physical interface velocity and the two closest neighbours velocity in the same phase. Then, if the left state is Ψ_l, the right state is defined by:

$$\Psi_r^{\text{prim}} = (2u_1^* - u_1, 2u_2^* - u_2, Y_{,1}^1, Y_{,1}^2, Y_{,2}^1, Y_{,2}^2, p, c). \tag{16}$$

In 2D, for both cases, a convex interpolation is performed between the state obtained to impose the boundary condition and an extrapolated fluid state Ψ_f^{prim} which is the solution of a Riemann problem in the tangential direction.

$$\Psi_{r,\text{final}}^{\text{prim}} = \alpha\Psi_r^{\text{prim}} + (1-\alpha)\Psi_f^{\text{prim}}, \quad \alpha = |n_\varphi . n_{\text{cell}}|$$

The weight α of the convex interpolation is the absolute value of the scalar product between the normal at the physical interface n_φ and the normal to the numerical interface n_{cell}, see Fig. 3.2, where the flux is currently calculated. Then, in the case of a physical interface parallel to the grid, we recover the 1D scheme, and in the case where the physical interface makes a big angle with the numerical interface, the boundary condition is not taken into account, see Fig. 3.2.

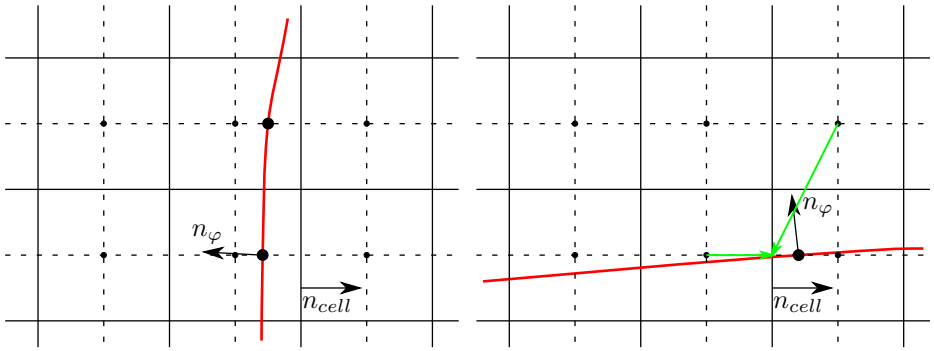

Figure 2: Geometrical configuration in the case α close to one and zero, for left and right respectively.

4 Results

In the following, we call "multimaterial scheme" a finite volume method with slopes reconstruction, using HLLC Riemann solver to compute the fluxes between cells belonging to the same material, and the HLLC multimaterial solver to compute the fluxes between cells belonging to different materials (the level set function φ changes sign). The scheme called "second order scheme" is the same but the multimaterial solver is replaced by the second order procedure described before.

4.1 1D test cases

We present a solid-solid shock tube with shear, see Fig. 3, this test case is also presented in [13]. We consider a shock tube filled with copper whose density is initially $\rho = 8.9.10^3 \text{kg/m}^3$. An interface separates the high pressure chamber on the left where the copper is at rest with pressure 10^9Pa and the same material on the right at low pressure (10^5Pa). A tangential velocity discontinuity is imposed: $u_2 = 0$m/s on the left and $u_2 = 100$m/s on the right. The interface is initially located at $x_i = 0.5$m. We consider a stiffened gas law with $\gamma = 4.22$ and $p_\infty = 3.42.10^{10}$Pa. The elastic coefficient $\chi = 5.10^{10}$. The grid is of 400 points and the CFL is 0.5, first and second order are compared to the exact solution obtained with the methods previously described. Five waves corresponding to a couple of shear waves, two normal stress waves and the contact discontinuity are present in the field. The fastest waves are those relative to the normal stress. The shear and the normal stress, the horizontal and the vertical speeds are continuous at the interface. The density and the pressure are continuous at the interface, and the interface is sharp.

The second order scheme at the interface has no visible effect in this case because the slopes for each variable in the cells neighbouring the physical interface are zero since the first iterations. However, the scheme is stable, accurate and oscillation-free.

4.2 2D test cases

In 2D, the level set function is transported at the flow velocity with a WENO5 method.

2D elastic-elastic. First, the 1D solid-solid shock tube with copper in presence of a tangential velocity is performed in 2D. The computational domain is $[-0.5, 1.5] \times [-0.5, 1.5]$. When the interface is exactly parallel to the grid (in x or y direction), we recover a 1D case and the results are those expected.

When the interface makes an angle with the grid, the test case is really 2D, and one can see numerical instabilities due to the geometric configuration when the interface crosses the grid.

As in 1D, slopes are in the limit zero at the interface, so the precision is expected to be close to the multimaterial scheme. But thanks to the convex interpolation between the boundary condition state and the extrapolated fluid state, we can recover a better regularity in the tangential direction.

On Fig. 5, the solution with 400 grid points in each direction is represented along a line normal to the interface passing through the center of the domain, and along a line parallel to the physical interface and located at 0.1 at both side of the interface.

2D fluid-fluid. A fluid/fluid 2D test case is performed: the propagation of a 1.22 Mach shock through a helium bubble in air, this test case were initially proposed in [14]. The computational domain is 890mm $\times$ 89mm, the helium bubble has a 50mm diameter and is initially located at (420mm, 44.5mm) and the initial position of the shock is 222.5mm away from the right side of the domain.

The multimaterial solver is used at the physical interface in the normal direction to determine the interface normal velocity. More precisely, a Riemann problem is defined at the intersection between the segment connecting the cell centers concerned by the sign change of the level set and the zero iso-line of the level set function by extrapolation of the slopes. Then, knowing the interface velocity, the scheme presented in [6] is applied at both side of the interface in order to impose this boundary condition at second order accuracy.

The simulation is in very good agreement with the litterature, see [15] for example. The interface stays sharp, and the scheme is second order accuracy.

5 Conclusion

We presented a simple and accurate method to deal with multimaterial interface. This method is based on a locally non conservative scheme which ensures that the contact discontinuity is kept sharp. We presented an analytical computation of the wave speeds and showed that the model is hyperbolic. A scheme originally developed to impose the non penetration boundary condition for the Euler equations is adapted to this model and validated with a solid-solid test case. The solution is compared to the solution obtained with an exact five-wave Riemann solver and it shown to be consistent. In two dimensions we showed that the new

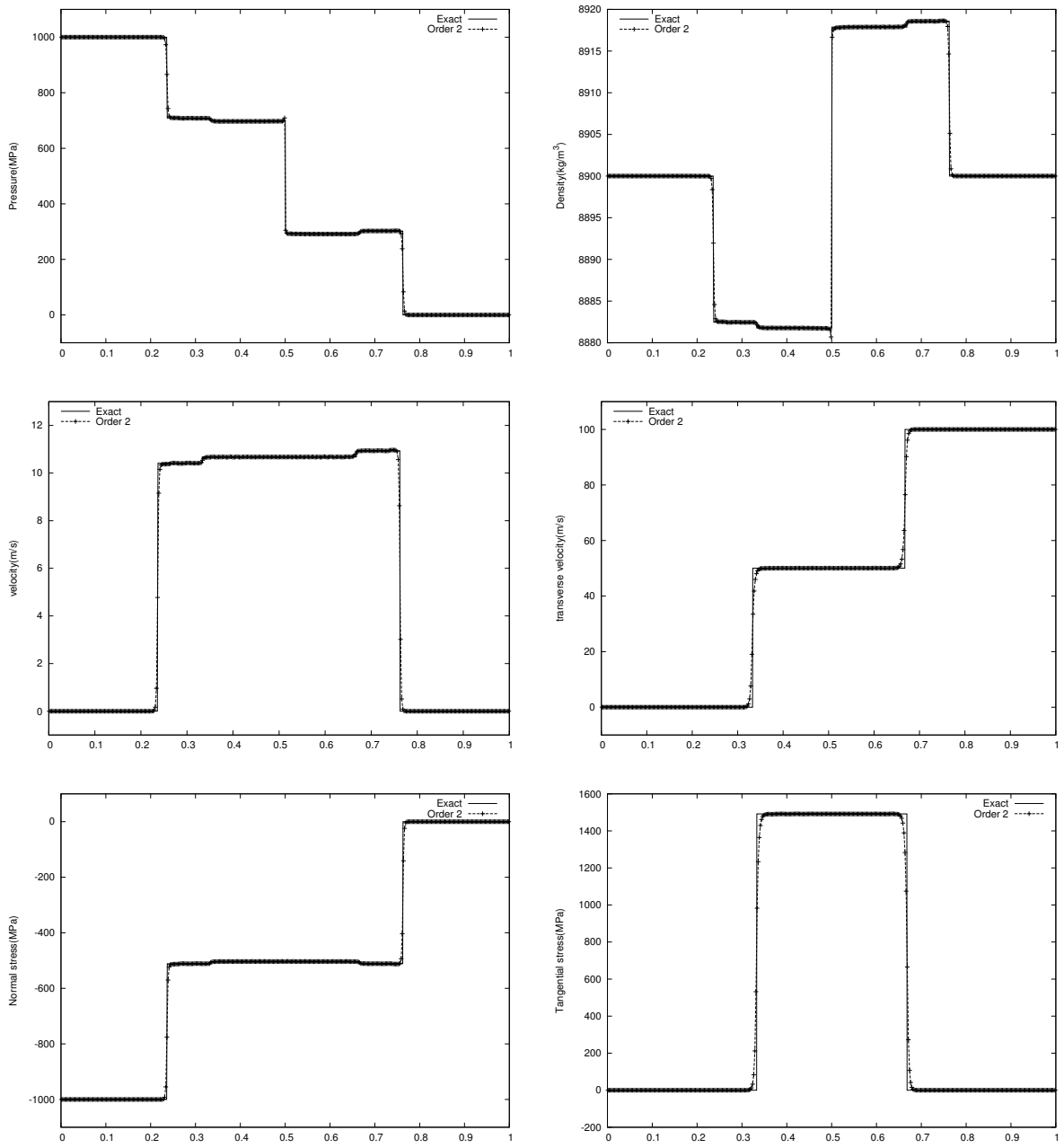

Figure 3: Results at $t = 5.10^{-5}$ for the solid-solid shock tube with copper in presence of a tangential velocity. Symbols represent our sharp interface method at second order with minmod slope limiter.

scheme improves the flow field for the elastic-elastic shock tube, and we obtained a good agreement with the literature for the shock bubble interaction test case. Future investigations concern the 2D fluid-elastic interaction.

Acknowledgement

This research is funded in part by the FP7 project FFAST, project ACP8-GA-2009-233665.

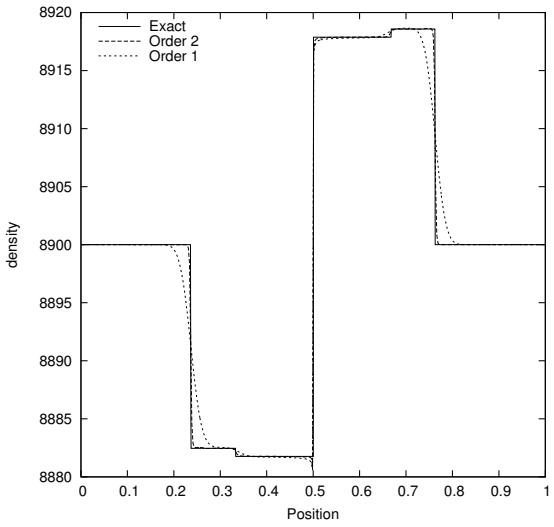

Figure 4: Comparison between order 1, order two and exact, for the solid-solid shock tube with copper in presence of a tangential velocity. The computation is performed on a 400 points grid for both.

References

[1] S.K. Godunov. Elements of continuum mechanics. *Nauka Moscow*, 1978.

[2] G.H. Miller and P. Colella. A high-order eulerian godunov method for elastic plastic flow in solids. *Journal of computational physics*, 167(1):131–176, 2001.

[3] R. Abgrall and S. Karni. Computations of compressible multifluids. *Journal of computational physics*, 169(2):594–623, 2001.

[4] S.L. Gavrilyuk, N. Favrie, and R. Saurel. Modelling wave dynamics of compressible elastic materials. *Journal of computational physics*, 227(5):2941–2969, 2008.

[5] A. Iollo, T. Milcent, and H. Telib. A sharp contact discontinuity scheme for multimaterial models. *Finite Volumes for Complex Applications VI. Springer Proceedings in Mathematics 4*, 2011.

[6] Y. Gorsse, A. Iollo, and L. Weynans. A simple second order cartesian scheme for compressible flow. *Finitie Volumes for Complex Applications VI. Springer Proceedings in Mathematics 4*, 2011.

[7] G.-H. Cottet, E. Maitre, and T. Milcent. Eulerian formulation and level set models for incompressible fluid-structure interaction. *M2AN*, 42:471–492, 2008.

[8] P.G. Ciarlet. *Mathematical elasticity Vol I, Three dimensional elasticity.* Volume 20 of Studies in Mathematics and its Applications, 1994.

[9] P.T. Barton, D. Drikakis, E. Romenski, and V.a. Titarev. Exact and approximate solutions of Riemann problems in non-linear elasticity. *Journal of Computational Physics*, 228(18):7046–7068, October 2009.

[10] E.F. Toro, M. Spruce, and W. Speares. Restoration of the contact surface in the hll-riemann solver. *Shock Waves*, 4:25–34, 1994.

[11] A. Chertock, S. Karni, and A. Kurganov. Interface tracking method for compressible multifluids. *ESAIM: Mathematical Modelling and Numerical Analysis*, 42:991–1019, 2008.

[12] B. Van Leer. Towards the ultimate conservative difference scheme i. the quest of monotonicity. *Lecture notes in Physics*, 18:163, 1972.

[13] N. Favrie, S.L. Gavrilyuk, and R. Saurel. Solid fluid diffuse interface model in cases of extreme deformations. *Journal of computational physics*, 228(16):6037–6077, 2009.

[14] James J Quirk and S Karni. On the dynamics of a shock-bubble interaction. *Journal of Fluid Mechanics*, 318(-1):129–163, 1996.

[15] Ronald P Fedkiw, Tariq Aslam, Barry Merriman, and Stanley Osher. A Non-oscillatory Eulerian Approach to Interfaces in Multimaterial Flows (the Ghost Fluid Method). *Journal of Computational Physics*, 152(2):457–492, July 1999.

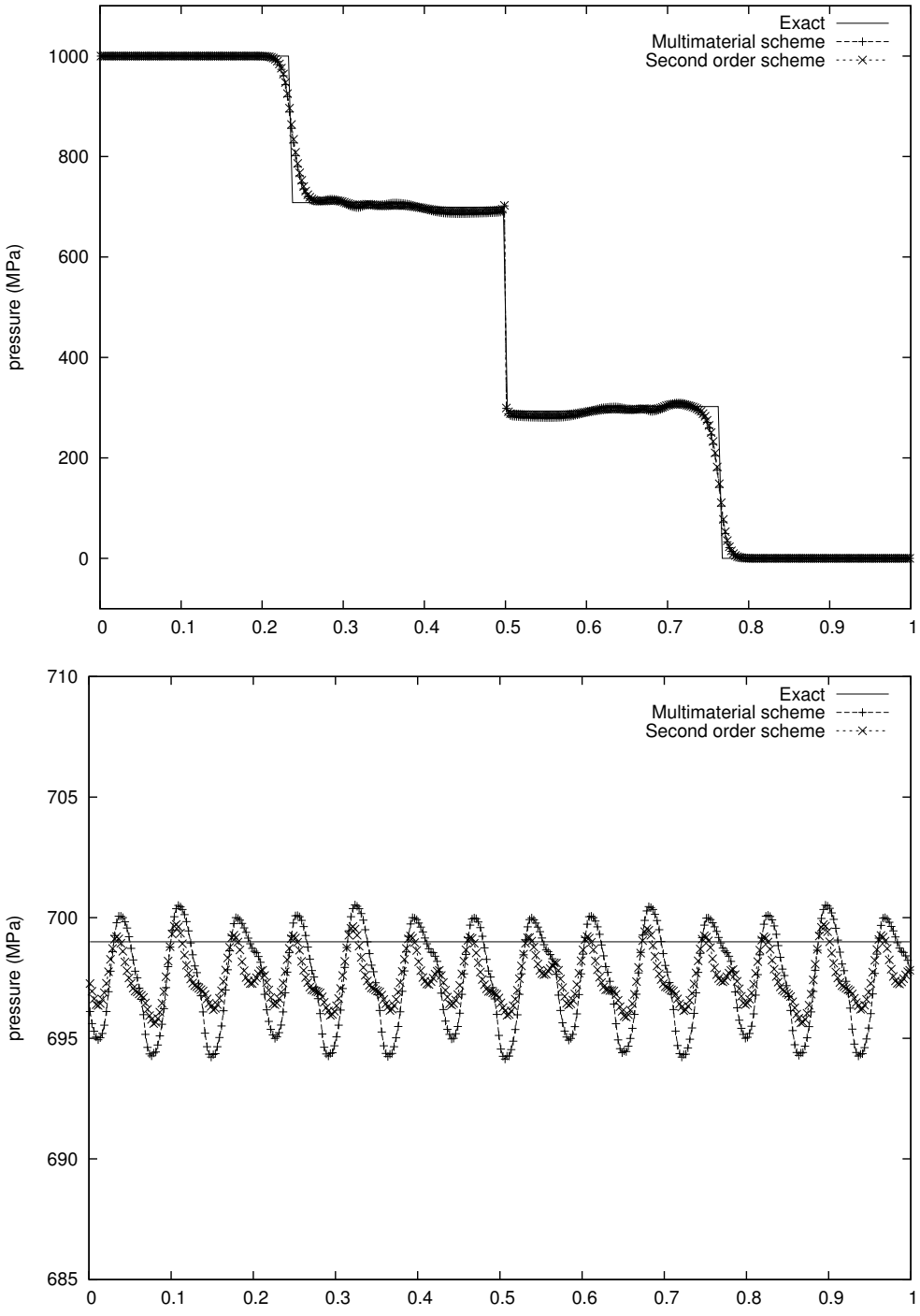

Figure 5: Solution at $t = 5.10^{-5}$ along a line normal to the interface at the top, and parallel to the interface at the bottom for the pressure. The dashed line is multimaterial scheme. The interface make an angle of 4° The convex interpolation in the 2D second order scheme improve the fields.

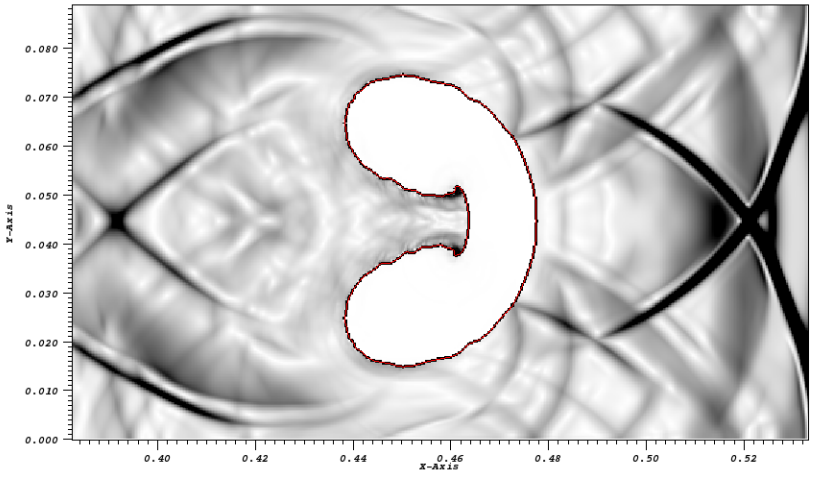

Figure 6: Schlieren image at t=400μs for the 2D test case.